Examining suspended sediment sources and dynamics during flood events in a drained catchment using radiogenic strontium isotope ratios ($^{87}Sr/^{86}Sr$)

Marion Le Gall[a*], Olivier Evrard[a], François Thil[a], Anthony Foucher[b], J. Patrick Laceby[a], Louis Manière[a], Sébastien Salvador-Blanes[b], Sophie Ayrault[a]

[a] *Laboratoire des Sciences et de l'Environnement, LSCE/IPSL, CEA-CNRS-UVSQ, Université Paris-Saclay, F- 91198 Gif-sur-Yvette, France*

[b] *E.A 6293, Laboratoire GéoHydrosystèmes Continentaux (GéHCO), Université F. Rabelais de Tours, Faculté des Sciences et Techniques, Parc de Grandmont, 37200 Tours, France*

Highlights

- Soil samples were discriminated according to catchment substrate (i.e. carbonate and silicate)
- $^{87}Sr/^{86}Sr$ ratios of suspended sediment varied depending on hydrological conditions
- Different particle size fractions were modelled for different flood intensities (i.e. <2 mm and <2 µm)
- Carbonate source soils dominated two less intense flood events (63%) whereas silicate source soils dominated a higher intensity flood (72%)
- Field drainage systems likely enhance the hillslope to river connectivity, particularly for the finest particles

Abstract

Soil erosion is recognized as one of the main processes of land degradation in agricultural areas. High suspended sediment loads, often generated from eroding agricultural landscapes, are known to degrade downstream environments. Accordingly, there is a need to identify suspended sediment sources and to investigate their dynamics. Here, soil and sediment strontium isotopic ratios were used to examine suspended sediment sources and dynamics in a lowland drained catchment in France.

Suspended sediment (n=14) was collected in stream and at tile drain (n=4) outlets during three flood events between December 2013 and February 2014. Potential source soils (n=28) representative of the carbonate and silicate substrates found in the catchment were sampled and analyzed. Strontium isotopic ratios ($^{87}Sr/^{86}Sr$) were measured in different particle size fractions (<2 µm, <63 µm and <2 mm).

Soil $^{87}Sr/^{86}Sr$ ratios significantly discriminated between source samples classified as carbonate (0.712625 to 0.717815) and silicate (0.719287 to 0.724631) soils. $^{87}Sr/^{86}Sr$ ratios measured in suspended sediment (0.713660 to 0.720571) reflect variations in source contributions during different hydrological conditions. The $^{87}Sr/^{86}Sr$ ratios varied in the different fractions of soil samples (i.e. <2 µm, <63 µm and <2 mm) and in suspended sediment samples. Suspended sediment was interpreted as a mixture of two end-members, with the dominant contribution of the <2 µm fraction of soil samples occurring during small scale flood events and the <2 mm fraction during more intense flood events. Modelling results indicate that carbonate source soil contributions are variable, with their highest contributions occurring during the two first flood events compared to the last flood event.

The results also show that the tile drainage system enhances the connectivity between cultivated hillslopes and the river network, providing a preferential pathway for fine (<2 µm) particles. This study demonstrates the potential of using strontium isotopic ratios to examine the variations of suspended sediment sources in drained catchments with contrasting carbonate and silicate sources. More importantly, the results highlight

the need to improve the management of sediment exported from tile drains in similar agricultural environments, as they were demonstrated to transfer very fine material to the riverine environment.

Keywords: $^{87}Sr/^{86}Sr$ ratio, suspended sediment, soil erosion, sediment tracing

1 Introduction

Accelerated soil erosion often results in elevated sediment loads (Owens et al., 2005). High sediment loads may lead to the siltation of river channels and reservoirs (Verstraeten and Poesen, 1999; Walling and Fang, 2003; Gay et al., 2014). These problems are exacerbated for the clay to loam fractions of sediment (typically <63 µm) that are transported the farthest from their sources. Importantly, fine sediment may also transport various contaminants, such as metals (Priadi et al., 2011), polycyclic aromatic hydrocarbons (Gateuille et al., 2014), nutrients (Beusen et al., 2005) and fallout radionuclides (Chartin et al., 2013).

There is a need to improve our understanding of sediment source dynamics in order to design effective sediment management programs. This is important for cultivated catchments of Northwestern Europe (Russell et al., 2001; Walling et al., 2002) where the intensification of agriculture after World War II resulted in an increase of sediment yields (Vanmaercke et al., 2015). In particular, knowledge of erosion processes and sediment sources is limited for catchments where tile drains were installed after the 1950s (Sogon et al., 1999; King et al., 2014). Drainage networks were installed in many agricultural catchments worldwide and although several studies suggest that the drainage system may increase the connectivity between cultivated hillslopes and the river network (Walling and Collins, 2008; Foucher et al., 2015), additional information is needed to characterize the source and nature of eroded material transported in these systems.

Eroded material is transported in rivers as suspended load or bedload, and rivers transport eroded material as both dissolved and particulate load. River monitoring is important for understanding sediment transport processes (Horowitz, 2008; Smith and Dragovich, 2009; Liu et al., 2011; Gourdin et al., 2014) or to estimate chemical mass budgets (e.g. Viers et al., 2009). In many cases, sediment fluxes and their associated contaminants are controlled by the occurrence of large flood events as demonstrated by numerous catchment-scale studies in which long time records are available (Audry et al., 2004; Coynel et al., 2007; Ollivier et al., 2011). Nevertheless, small agricultural catchments with extensive drainage networks, where significant suspended sediment export occurs during small and medium sized flood events, have received limited attention. Accordingly, investigating sediment sources in small drained agricultural catchments may provide insight into fundamental hydrological and erosion processes.

Sediment provenance can be determined by analyzing the sediment geochemistry of river material that is essentially a mixture between its lithological and pedological sources (Collins et al., 2010; Evrard et al., 2011). In addition to the analysis of major and trace elements, targeted isotopic ratios are a powerful tool to discriminate the contributions of potential sediment sources. This ability was demonstrated for strontium isotopes (^{87}Sr and ^{86}Sr) that are not fractionated during weathering processes (dissolution of primary minerals and precipitation of secondary phases). Although the bedrock $^{87}Sr/^{86}Sr$ ratio depends on the Rb/Sr ratio of the constitutive minerals and age (Faure, 1986; Albarède, 1995), the minerals neoformed during their transformation in soils should maintain their bedrock strontium isotopic signatures (Graustein, 1989; Douglas et al., 1995).

As a consequence, ^{87}Sr and ^{86}Sr isotopes have been extensively used to investigate weathering and erosion processes (Négrel et al., 1993; Gaillardet et al., 1997; Probst et al., 2000; Semhi et al., 2000; Pierson-Wickmann et al., 2009; Brennan et al., 2014) and for tracing river water masses (Eikenberg et al., 2001; Brenot et al., 2008; Bouchez et al., 2011a). Few studies have reported variations of $^{87}Sr/^{86}Sr$ ratios during floods in large rivers in both dissolved (Négrel et al., 1993; Grosbois et al., 1999; Roy et al., 1999; Négrel and Petelet-Giraud, 2004; Petelet-Giraud and Négrel, 2007) and particulate loads (Douglas et al., 1995; Allègre et al., 1996; Asahara et al., 1999). These latter studies demonstrated the potential of $^{87}Sr/^{86}Sr$ ratios to

discriminate sediment sources in riverine environments in general, and to discriminate between carbonate and silicate sources or between shield and volcanic terranes in particular.

The objective of this study is to investigate the sources of suspended sediment and to quantify their dynamics in the Louroux catchment (France), a small agricultural catchment representative of lowland drained areas of Northwestern Europe. In this catchment, the installation of dense drainage systems were shown to increase the connectivity between eroded soils and the river network, with the preferential transfer through the drains of very fine particles originating from the soil surface to the river network (Foucher et al., 2014).

To improve our understanding of suspended sediment sources in this drained and intensively cultivated catchment, $^{87}Sr/^{86}Sr$ and chemical element ratios were measured in suspended sediment during three flood events and three particle size fractions in potential source soil samples (i.e. <2 mm, <63 µm and <2 µm fractions). The objective of these measurements is to identify the sources supplying sediment to the river network and to examine their potential variations during a sequence of flood events. Accordingly, geochemical variations were examined according to hydrological conditions, suspended sediment end-members were identified, and the respective contribution of each end-member was estimated for each flood event.

2 Material and methods

2.1 Study site

The Louroux catchment (24 km²) is a small agricultural catchment located in the central part of the Loire river basin, France (Fig. 1A). It is characterized by a relatively flat topography (mean slope of 0.4%; elevation ranging between 99 and 127 m). The climate is temperate oceanic, with a mean annual rainfall of 684 mm (between 1971 and 2000) (Météo France). Cropland (intensive cereal production) is the main land use (78%) followed by grassland (18%) and woodland (4%) (European Environment Agency, 2002). Organic and mineral fertilizers are commonly used in the catchment. The geology exclusively consists of continental and marine sedimentary rocks. Six different lithologies are found in this lowland catchment (Fig. 1B) although they crop out at very limited locations. Senonian flint clays (23%) constitute the oldest and deepest formation. Tertiary detrital formations, as Eocene silicic conglomerate (2%), are found in the middle of the basin. Ludian Touraine lacustrine limestone (6%) is found in the western part of the catchment where it is covered with Helvetian shelly sands (18%). Post-Helvetian sand and continental gravel (32%) cover the largest area and result from fluviatile spreading. Quaternary loess (18%) covers tertiary deposits in the upstream part of the catchment (Rasplus et al., 1982). These lithologies were regrouped in two classes: a carbonate area composed of Touraine lacustrine limestone, Helvetian shelly sand and Post-Helvetian sand and continental gravel, and a silicate area comprising the remaining lithologies (Fig. 1C). Importantly, the carbonate substrates were predominately located in the southern part of the catchment. According to the Food and Agriculture Organization classification (World Reference Base for Soil Resources, 2006), most of the soils are hydromorphic soils classified as Neoluvisols and prone to surface crusting except in the southern part of the catchment where Calcosols and Calcisols overlie the Touraine lacustrine limestone.

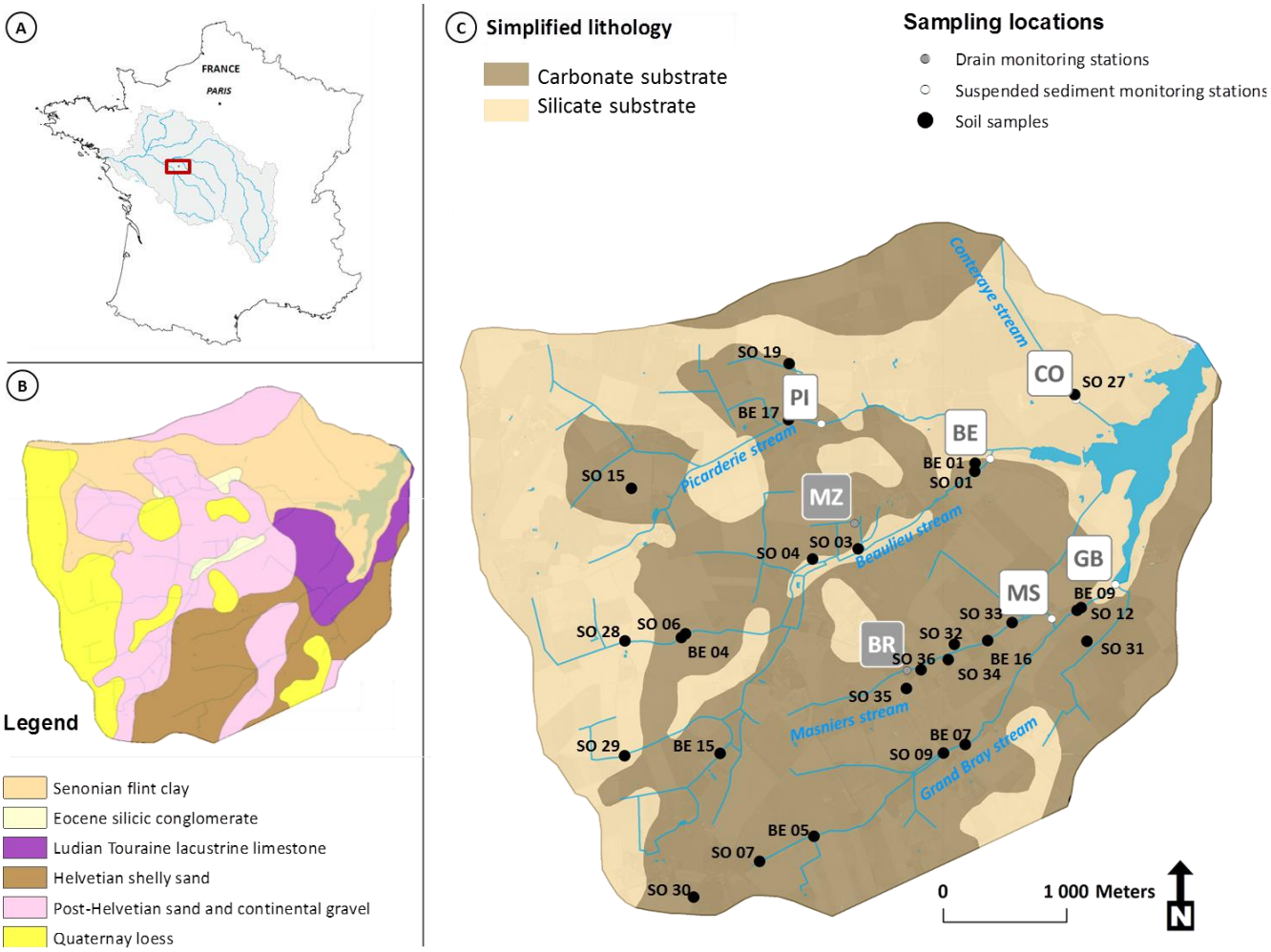

Figure 1. Map of the Louroux catchment in the Loire River basin (France) (A) along with the lithological map of the area (B) and the locations of soil sampling, river monitoring stations equipped with automatic samplers (in white) and tile drain outlet monitoring stations (in grey) (CO: Conteraye, BE: Beaulieu, PI: Picarderie, GB: Grand Bray, MS: Masniers, MZ: Mazère, BR: Brépinière) (C). For the soil samples, SO refers to surface samples and BE refers to channel bank samples.

Large-scale modifications of land use and agricultural practices took place in the Louroux catchment over the last 70 years. A succession of land consolidation schemes was implemented in the area, which modified the river network and installed a dense tile drain system to evacuate stagnating water. More than 220 tile drain outlets were installed throughout the catchment to drain the soils. These modifications led to increased sediment yields (maximal value of 1100 t km^{-2} yr^{-1} during the 1960-1980 period) in the Louroux Pond (0.5 km^2), located at the catchment outlet (Foucher et al., 2014). Five main streams drain to the Louroux Pond: the Conteraye, Picarderie, Beaulieu, Masniers and Grand Braye streams. The main flow direction is from the western to the eastern part of the catchment, where the pond is located (Fig. 1C).

2.2 Sampling

2.2.1 Source collection

Soil and channel bank samples (respectively referred to as SO and BE in Fig. 1C) were collected between January 2013 and April 2014 in cropland areas. Surface sources (n=20) were sampled by scraping the top 2-3 cm layer of soil. Channel bank sources (n=8) were sampled by scraping a 2-3 cm layer of the sidewall from eroding channel banks. A plastic spatula was used to collect these samples to avoid potential contamination.

Source samples were composed of three to five sub-samples, all collected within a radius of 10 m. During sampling, care was taken to cover soils corresponding to the range of substrates found in the catchment.

2.2.2 Suspended sediment collection

Five monitoring stations (CO, PI, BE, MS, GB stations in Fig. 1C) equipped with automatic samplers containing twenty-four 1L polypropylene bottles were installed on five streams draining to the Louroux Pond. For each monitoring site and each flood, one acid-cleaned 1L polypropylene bottle was dedicated for geochemical analyses. In addition to the river monitoring sites, two stations were installed at tile drain outlets to characterize the properties of the sediment transiting through the drainage system. Suspended sediment exported from drains (BR, MZ stations) was collected in the same way as suspended sediment in the rivers. Water level and turbidity were continuously recorded at the seven monitoring stations to estimate water discharge and suspended sediment concentrations. For the flood events investigated, data were available for four of the monitoring stations (BR, GB, MS for the three floods and BE for the two first floods). Three flood events were investigated (December 30, 2013, January 29, 2014 and February 13, 2014). Eighteen samples of river water were collected for geochemical analyses, including fourteen in the river monitoring stations and four at tile drain outlets. For each flood, one sample of river water was collected at the beginning of the recession stage of the hydrograph. During the two first floods, samples were collected at every station (5 river and 2 tile drain samples) for each event. During the last flood, samples were only collected at 4 river monitoring stations (excluding the CO and BR and MZ tile drain stations).

2.3 Sample processing and analysis

2.3.1 Sample preparation

In the laboratory, soil samples were dried at 40°C and sieved to 2 mm before analysis. The <63 µm and <2 µm particle sizes were fractionated for a selection of soil samples (n=8). Sieving sediment source material to <63 µm facilitates the direct comparison of its properties with those of suspended sediment, as it is widely accepted that fine material (typically <63µm) is preferentially transported in suspension (Koiter et al., 2013; Smith and Blake, 2014). Furthermore, the <2 µm fraction containing the clay minerals was separated. The <63 µm fraction was isolated by dry sieving and settling columns were used to isolate the <2 µm fraction by sedimentation using deionized water. The larger particles (i.e >2 µm) were expected to have settled after a given period calculated using Stokes' law. A fall distance of 3 cm was calculated for the <2 µm fraction on the basis of a constant temperature of 20°C and a density of 2.65 g cm^{-3}. After 140 minutes, the supernatant solution with particles <2 µm was removed and dried at 40°C. Suspended sediment concentrations were determined by the filtration of a known volume of water (120 mL to 900 mL) through dried, acid-cleaned and pre-weighted glass fiber filters (Whatman, GF/F, 47 mm Ø, 0.7 µm pore size). Suspended sediment quantities collected on the filters ranged from 59 to 347 mg (weighing error: <3%).

2.3.2 Geochemical measurements

Bulk mineralization

Approximately 100 mg of soil and channel bank material were dissolved with 3 mL HF (47-51%) and 3 mL $HClO_4$ (65-71%) in closed Teflon vessels under pressure on hot-plates at 150°C for 240 min (Digiprep, SCP Science protocol). After cooling, solutions were evaporated to dryness. Samples were then digested using aqua regia: 3.75 mL HCl (34-37%) and 1.25 mL HNO_3 (67%) at 110°C for 120 min (Digiprep SCP Science

186 protocol). Solutions were then evaporated to dryness. Finally, samples were dissolved and evaporated
187 successively three times in 1mL of HNO_3 (67%) and diluted in 50 mL of ultrapure water (Milli-Q). Ultrapure
188 reagents were used (Normatom grade, VWR, France for HNO_3, and "Trace Metal Grade", Fisher Chemical,
189 France for HF, $HClO_4$ and HCl) and for each set of total digestion, a reference material (IAEA lake sediment
190 SL1) and a chemical blank were digested in the same way to control chemical mineralization efficiency.

191 Prior to digestion, dried, weighted suspended sediment filters were cut into two parts using ceramic scissors.
192 Half of each filter (between 50 and 110 mg) was digested in closed Teflon vessels using the same procedure
193 as described above. For each batch of total digestions, a clean filter was digested in the same way as the
194 samples to check for any potential contamination.

195 *Determination of major and trace element concentrations*

196 Major and trace element concentrations (Na, Mg, K, Ca, Al, Rb, and Sr) were determined in digested solutions
197 using an inductively coupled plasma quadrupolar mass spectrometer (ICP-QMS) (X-Series, CCT II^+
198 Thermoelectron, France). Internal standards (Re, Rh and In; SPEX, SCP Science, France) were used to correct
199 for instrumental drift and plasma fluctuation. To limit interference, analysis was performed using a collision
200 cell technology (CCT) which introduces a supplementary gas mixture of H_2 (7%) and He (93%) for the
201 determination of Rb and Sr concentrations.

202 A certified river water sample (SRM 1640a, NIST, Gaithersburg, USA) was used to control the ICP-QMS
203 calibration. The overall quality of the digestion procedure and of ICP-QMS measurements was controlled by
204 analyzing a certified lake sediment material (SL-1, International Atomic Energy Agency, Vienna). These
205 standards were analyzed routinely (every 15-25 samples). Good agreement was observed between the data
206 obtained and the certified values (n=91 for SL-1 measurements). In the particulate compartment, analytical
207 uncertainties did not exceed 10% (except for Ca, with a maximal analytical error of 13%). In the blank filter,
208 major and trace element concentrations did not exceed 2% of the concentrations measured in suspended
209 sediment, except for Na measurements which had a maximum contribution of 8%.

210 *Sr purification and isotopic measurements*

211 Chemical separation of Sr from Rb and Ca was performed using a cation-exchange procedure. A Sr specific
212 resin was used (Sr-SPEC resin, Eichrom) and packed on lab-made polyethylene microcolumns (700 µL resin).
213 After the bulk digestion, a calculated volume of each sample, equivalent to 200 ng of Sr in 4 mL HNO_3 3N, was
214 prepared. The resin was conditioned three times with 25 mL of HCl 1N and 25 mL of HCl 3N to remove
215 potential traces of Sr and Pb, and then rinsed with ultrapure water (Milli-Q) until pH 6-7 was reached. The
216 resin was then loaded onto pre-cleaned extraction chromatographic microcolumns and rinsed successively
217 with 2 mL of HNO_3 3N, 2 mL of ultrapure water (Milli-Q) and 1mL of HNO_3 3N. Digestion solutions (containing
218 200 ng of Sr) were then loaded onto columns. Sr elution was realized using 3 mL of HNO_3 3N and 2.5 mL of
219 ultrapure water (Milli-Q). Sr recovery (measured to 85%, σ=11.5%, n=129) and efficiency of purification were
220 determined by comparing the Sr and Ca concentrations in the original digest (after the bulk digestion) and in
221 the eluted Sr fraction. More than 90% of the Ca was eliminated after the chemical extraction.

222 Sr isotope ratio analyses were carried out using a Thermo Finnigan Neptune-Plus Multi-collector Inductively
223 Coupled Plasma Mass Spectrometry (MC-ICP-MS) instrument at the Laboratoire des Science du Climat et de
224 l'Environnement. The purified Sr fractions obtained after chemical separation were diluted with 0.5N HNO_3,
225 adjusting the Sr concentration to 20 µg/L. Reproducibility of the $^{87}Sr/^{86}Sr$ ratio measurements was controlled
226 with replicate analyses of the NBS 987 standard, the mean value obtained was $0.710304 \pm 11x10^{-6}$ (2σ, n=88).
227 Ratios obtained were normalized to the NBS 987 standard value of 0.710245 and $^{86}Sr/^{88}Sr$=0.1194 was

adopted to calibrate mass bias during the Sr isotope measurements. Two other standards were also used, the JCt-1 (carbonate mineral, accepted value of 0.709150) and the Durango apatite (accepted value of 0.706327). Recalculated mean values, normalized to the NBS 987, obtained were respectively 0.709267 ± 11x10^{-6} (2σ, n=18) and 0.706346 ± 13x10^{-6} (2σ, n=24).

2.4 Source discrimination analyses and modelling

Suspended sediment samples were hypothesized to derive from two source end-members reflecting the mixing of particles originating from source soils developed on carbonate and silicate substrates. To facilitate the presentation or results and discussion, these endmembers will be further referred to "carbonate soils" and "silicate soils".

Non-parametric tests were used to determine whether isotope ratios were significantly different in suspended sediment and in soil samples (Collins et al., 1997; Laceby et al., 2015). The non-parametric Mann-Whitney *U*-test was used to examine differences and similarities between suspended sediment sources and suspended sediment samples at a significance level of $p<0.05$.

To quantify the relative contribution of the sources (i.e., carbonate soils vs silicate soils) to suspended sediment samples, $^{87}Sr/^{86}Sr$ ratios and Sr concentrations were incorporated in the following equation (Eq. 1):

$$R_{SS} = \frac{x_c . C_c . R_c + x_s . C_s . R_s}{x_c . C_c + x_s . C_s} \quad \text{(Eq. 1)}$$

where R_{SS}, R_C, R_S are the respective $^{87}Sr/^{86}Sr$ ratios in suspended sediment, carbonate and silicate soil samples; C_C and C_S are the respective Sr concentrations in carbonate and silicate soil samples; and x_C and x_S (with $x_C + x_S = 1$) are the respective carbonate and silicate contributions to suspended sediment.

Carbonate and silicate soil contributions to suspended sediment were estimated by minimizing the difference between the $^{87}Sr/^{86}Sr$ ratio measured in each suspended sediment sample by MC-ICP-MS and the $^{87}Sr/^{86}Sr$ ratio (R_{SS}) calculate following (Eq. 1).

For the two first flood events, $^{87}Sr/^{86}Sr$ ratios and Sr concentrations measured in the <2 µm fraction were incorporated in the mixing equation while for the third flood event, measurements in the <2 mm fraction were used. Both end-members were characterized by the mean value of the $^{87}Sr/^{86}Sr$ ratios and Sr concentrations measured in the carbonate and silicate soils.

3 Results

3.1 Spatial variations of $^{87}Sr/^{86}Sr$ ratios in source samples

A range of $^{87}Sr/^{86}Sr$ ratios was observed in source samples collected within the Louroux catchment. The $^{87}Sr/^{86}Sr$ ratios varied between 0.712625 and 0.722685 in channel bank samples (n=8), and between 0.712763 and 0.724631 in soil samples (n=20) (Fig. 2, Supplementary Table S1). A Mann-Whitney *U* test reported the absence of significant differences between these two sources (MW $p=0.355$). Accordingly, channel bank and soil samples were not considered as distinct sources.

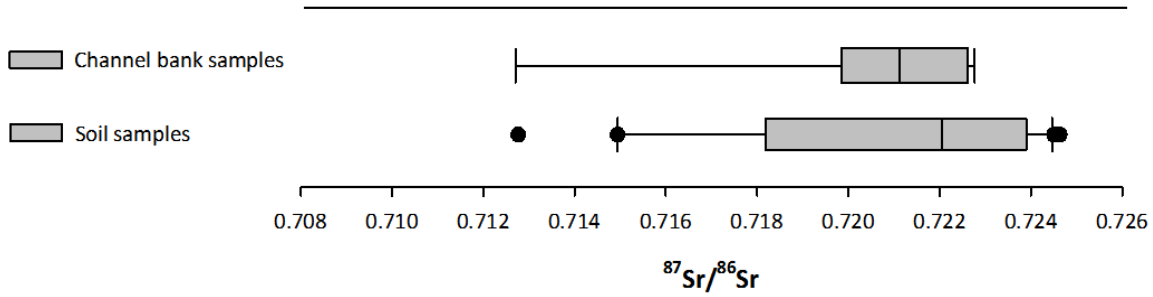

Figure 2. Box-plots of Sr isotopic ratio variations in channel bank and soil samples.

The lowest ratios (0.712625 to 0.719287) were observed in the carbonate area drained by Masniers and Grand Bray streams, in the southern part of the Louroux Pond catchment (Fig. 3, Supplementary Table S1) whereas intermediate (0.719651-0.722700) and higher ratios (0.722701-0.724631) were observed in the remaining areas.

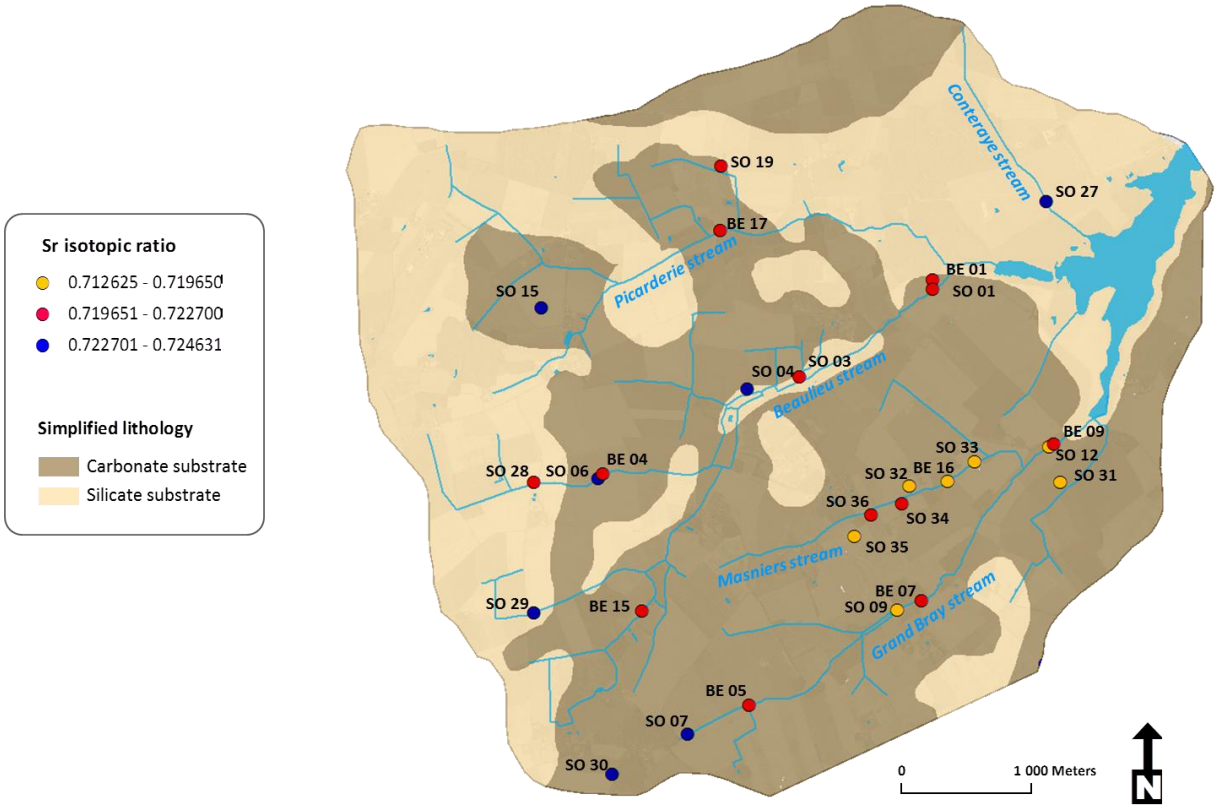

Figure 3. Location and $^{87}Sr/^{86}Sr$ ratios of soil and channel bank samples. For the soil samples, SO refers to surface samples and BE refers to channel bank samples.

3.2 Hydrological and geochemical characterizations of suspended sediment samples

Hydro-sedimentary parameters (i.e. water levels, turbidity) recorded during the 2013-2014 winter season were used to estimate the water discharge and suspended sediment concentration values. Unfortunately, they were only available for three monitoring stations (BE, GB, MS stations). The two first flood events were triggered by long-lasting and low-intensity rainfall and were characterized by similar suspended sediment concentrations. Water discharge recorded during the second flood were slightly lower that those recorded during the first flood, with respective maximal water discharge values of 0.76 and 0.42 $m^3 s^{-1}$ (GB station). On December 30, 2013, total precipitation reached 14 mm in 24 hours and suspended sediment concentrations

varied between 15 and 624 mg L^{-1}. On January 29, 2014, total precipitation reached 9.4 mm in 29 hours and suspended sediment concentrations varied between 2 and 416 mg L^{-1}. In contrast, the third flood event that occurred on February 13, 2014 was triggered by higher precipitation (21.6 mm in 4 hours) and was more intense with higher suspended sediment concentrations and water discharge, reaching the maximal values of 2450 mg L^{-1} and 1.1 m^3 s^{-1}, respectively, at the BE station. Due to the higher cumulative precipitation recorded during the previous months, soils were saturated with water. The more intense rainfall event that occurred on February 13, 2014 generated erosion and sediment transport, which is illustrated by the higher water discharge and suspended sediment concentrations recorded in the river during the third monitored flood event. Suspended sediment concentrations were highly variable from one flood to another, and clockwise hysteresis was observed for the three flood events (Fig. 4). Indeed, for a given discharge, suspended sediment concentrations were higher during the rising limb compared to the falling limb.

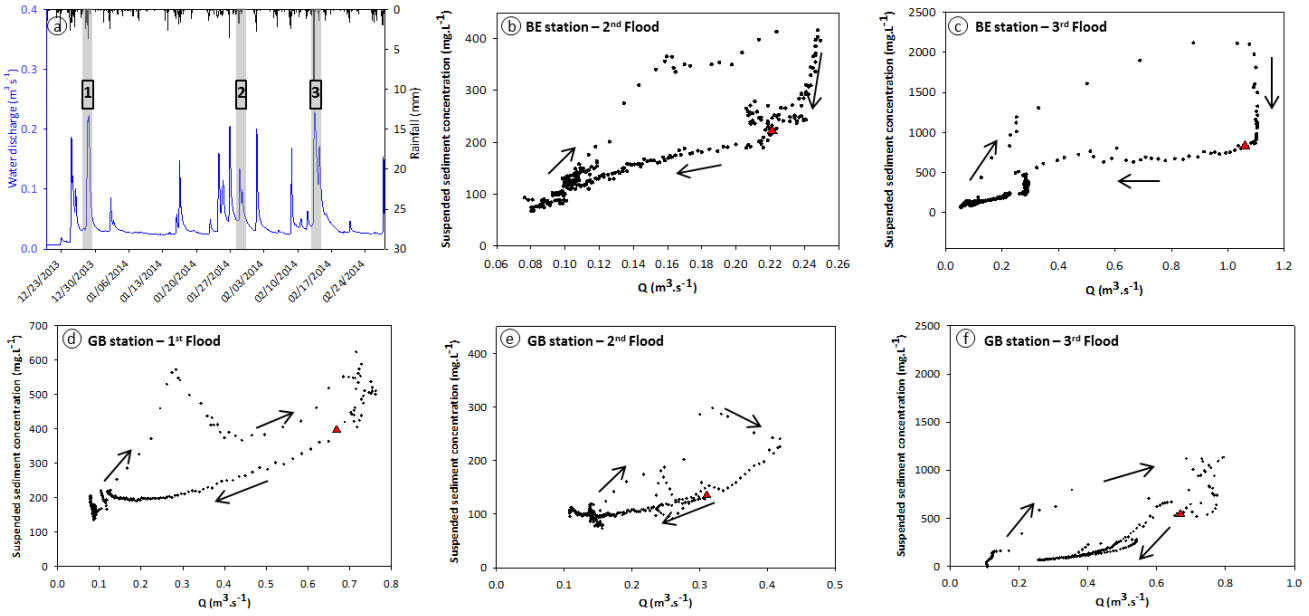

Figure 4. Water discharge and precipitation measured at the MS station during the December 2013 to the February 2014 period. Discharge and suspended sediment concentrations for the three flood events at two monitoring stations, BE and GB located in the silicate and carbonate areas and flowing to the Louroux pond. Samples collected for Sr isotopic measurements are noted by the red triangle. Data presented were respectively recorded during three days for the two first flood events and during four days for the third flood event.

During the three flood events, $^{87}Sr/^{86}Sr$ ratios measured in suspended sediment directly collected in the river and at tile drain outlets displayed large variations, with values ranging between 0.713660 and 0.720571 (Supplementary Table S2). Nevertheless, they remained within the source soil range (0.712736 to 0.724631). The two first flood events exhibited similar ranges of Sr isotopic variations with ratios between 0.713660 and 0.718637. The third flood event was characterized by higher ratios ranging from 0.717814 and 0.720571 (Supplementary Table S2). For each monitoring station, $^{87}Sr/^{86}Sr$ ratios measured in suspended sediment collected during the third flood were systematically higher than those measured during the two previous floods (i.e. from 0.718637 to 0.720571 at PI station, from 0.718188 to 0.720495 at BE station, from 0.715671 to 0.717814 at MS station and from 0.716165 to 718467 at GB station).

Similarly to the sources, the lowest $^{87}Sr/^{86}Sr$ ratios were measured in suspended sediment collected in the streams (n=6) and at tile drain outlets (n=2) draining the carbonate areas (0.715484 to 0.718467 and 0.713660 to 0.714202, respectively) mainly found in the southern part of the catchment, whereas the highest ratios were measured in suspended sediment (n=5) and at tile drain outlets (n=2) collected in the silicate area

(0.715734 to 0.720571 and 0.717296 to 0.717946, respectively). The two lowest ratios were measured at the tile drain outlet of the BP station during the two first flood events whereas the two highest values were measured in the samples collected during the third flood at the monitoring stations of BE and PI, both located in the vicinity of the silicate area. For each flood and each drained area, $^{87}Sr/^{86}Sr$ ratios measured in suspended sediment collected at tile drain outlets were systematically lower than those measured in suspended sediment directly collected in the stream (Supplementary Table S2).

3.3 Relationship between $^{87}Sr/^{86}Sr$ and elemental ratios in source and suspended sediment samples – end-member selection

A Hierarchical Cluster Analysis (HCA) was performed using $^{87}Sr/^{86}Sr$ ratios, Na, Mg, K, Ca, Rb and Sr concentrations measured in channel bank and soil samples. The results indicate that source samples can be grouped in two major clusters (Fig. S1). The first cluster (Group 1, n=4) contains samples with the highest Ca and Sr concentrations and $^{87}Sr/^{86}Sr$ ratios ranging between 0.712625 and 0.716986. These samples (SO31, SO32, SO33, BE16) are all located in the carbonate/southern area of the catchment. The second cluster (Group 2, n=24) is divided into several sub-clusters. In these samples, $^{87}Sr/^{86}Sr$ ratios are generally higher and Ca and Sr concentrations are lower than in samples of the first group. Their Na, Mg, K and Rb concentrations are variable.

To improve the discrimination of suspended sediment sources, the variations of $^{87}Sr/^{86}Sr$ and elemental ratios were investigated using scatter plots (Fig. 5). Soil and suspended sediment samples exhibited large variations in $^{87}Sr/^{86}Sr$ and chemical element ratios, suggesting that they were supplied by contrasting soil sources. High Ca/Sr combined with low K/Sr, 1/Sr, Rb/Sr and Na/Sr ratios indicated a carbonate component whereas low Ca/Sr associated with high K/Sr, 1/Sr, Rb/Sr and Na/Sr ratios were indicative of a silicate component. The first group of soil samples (SO31, SO32, SO33, BE16) displayed contrasting $^{87}Sr/^{86}Sr$ and elemental ratios compared to those of the second cluster. Furthermore, two additional source samples (SO12, SO35) from the second cluster indicated by a red arrow in Fig. 5 exhibited $^{87}Sr/^{86}Sr$ and elemental ratio values comparable to those of the soil samples from the first cluster.

These six soil samples (BE16, SO12, SO31; SO32, SO33 and SO35, represented with black circles on Fig. 5) were discriminated from the remaining soil samples and characterized by lower $^{87}Sr/^{86}Sr$, K/Sr, 1/Sr, Rb/Sr and Na/Sr ratios (Fig. 5a,c,d) and higher Ca/Sr ratios (Fig. 5b,e). Mg/Sr ratios did not discriminate between the two sources as the mean Mg/Sr ratios estimated in carbonate soils and silicate soils were similar. These six soil samples displayed the lowest $^{87}Sr/^{86}Sr$ ratios (between 0.712625 and 0.717815) suggesting a higher carbonate component compared to the remaining soil samples. Consequently, they were classified as carbonate soil samples and the remaining samples as silicate soil samples.

Suspended sediment samples did not plot along a mixing line between the carbonate and silicate soil source samples with the exception of suspended sediment from the third flood event that plotted with soil samples using Rb/Sr ratios (Fig. 5d). The $^{87}Sr/^{86}Sr$ ratios therefore were measured in the <63 µm and <2 µm fractions of select soil samples (n=8) (Supplementary Tables S3-4-5). The $^{87}Sr/^{86}Sr$ ratios in the <63 µm fraction (0.716178-0.724667) were slightly higher than in the <2 mm fraction but elemental ratios were slightly lower or higher depending on soil samples. Suspended sediment samples did not match with the <63 µm fraction of soil source samples. However, $^{87}Sr/^{86}Sr$ ratios in the <2 µm fraction were even lower than in the <63 µm fraction, with ratios ranging between 0.713099 and 0.722535 and suspended sediment samples plotted with the <2 µm fraction of soil samples using K/Sr, Ca/Sr, 1/Sr, Rb/Sr and Mg/Sr elemental ratios. This was not observed

for Na/Sr ratios which have very high values (524-1170) and were thus enriched Na concentrations in the <2um fraction relative to the other samples.

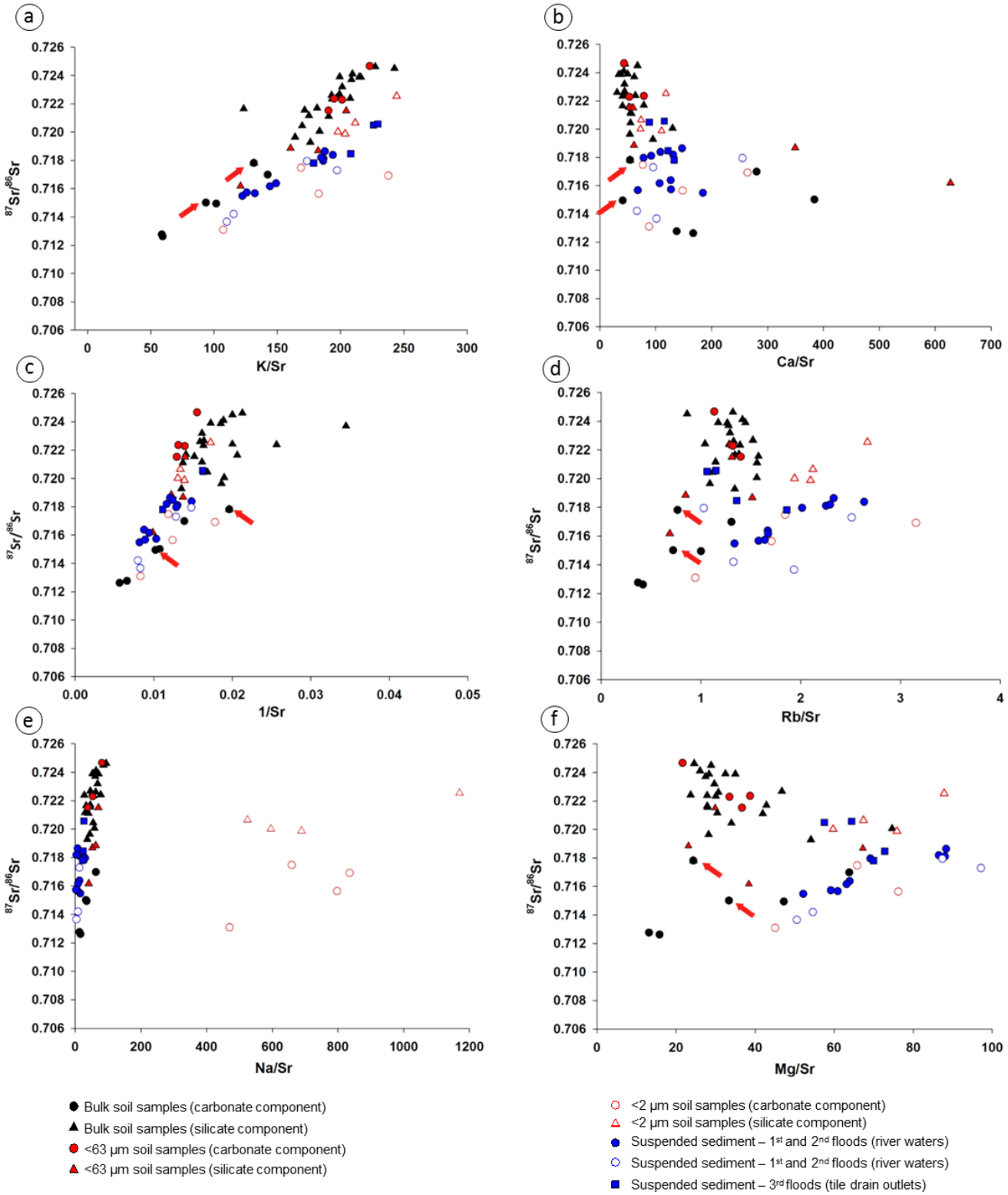

Figure 5. $^{87}Sr/^{86}Sr$ vs K/Sr (a), Ca/Sr (b), 1/Sr (c), Rb/Sr (d), Sr/Na (e) and Mg/Sr (f) for suspended sediment,<2 mm, <63 µm and <2 µm fraction of soil samples. Red arrows indicate the two soil additional soil samples used to define the carbonate end-member using scatter plots.

3.4 Preliminary quantification of source contributions to suspended sediment

In this cultivated catchment, results indicated that Sr isotopic signatures varied according to the particle size fraction analyzed (i.e. <2 mm, <63 µm and <2 µm). Accordingly, suspended sediment may be interpreted as a mixture of two end-members characterized by different source soil particle size fractions depending on the flood intensity.

Sr isotopic signatures significantly discriminated between the <2 mm fraction of soil samples and suspended sediment from the two first flood events (MW p=0.000) though not the last flood event (MW p=0.172). This suggests, in combination with the figures above (Fig. 3 and Fig. 5), that the <2 mm fraction of soil samples could be used as a source of suspended sediment during the last flood event. Mann-Whitney tests were then performed to assess the ability of $^{87}Sr/^{86}Sr$ ratios to discriminate between the <2 mm fraction of soil samples and the <63 and <2 µm fractions, respectively. Results reported the absence of significant differences between the <2 mm and <63 µm fractions (MW p=0.115) but they showed significant differences between the <2 mm and <2 µm fractions (MW p<0.042). Furthermore, no significant difference was observed between the <2 µm fraction of soil and suspended sediment collected during the two first flood events (MW p=0.242). These results suggest that the <2 µm and the <2 mm fraction of soil samples should be modelled as suspended sediment sources depending on hydrological conditions in the Louroux catchment as they control the particle size fractions transported in suspension.

As $^{87}Sr/^{86}Sr$ ratios measured in soil samples reflect the mixing of carbonate and silicate source soils, the respective contributions of these two end-members to the suspended sediment were modelled (Eq. 1). $^{87}Sr/^{86}Sr$ ratios and Sr concentrations measured in the <2 µm and in the <2 mm fractions of soil samples were used to respectively investigate end-members contributions during the two first flood events and during the third flood event.

Table 1. Mean and Standard Deviation for Sr isotopic signatures, Sr concentrations (mg kg^{-1}) for the different end-members.

	End-Members	$^{87}Sr/^{86}Sr$	Sr
<2 µm Fraction	Carbonate soil samples	0.715222 ± 7	86 ± 7
	Silicate soil samples	0.720113 ± 8	73 ± 6
<2 mm Fraction	Carbonate soil samples	0.715024 ± 8	107 ± 9
	Silicate soil samples	0.722316 ± 17	55 ± 4

Results (Fig. 6a,b,c) indicate that carbonate soil contributions were the highest during the two first flood events when the <2 µm fraction contributed to suspended sediment (mean carbonate contributions of 61% and 65%) compared to the third flood where the <2 mm fraction of silicate soils contributed the highest proportions to the suspended sediment (mean silicate contribution of 72%) (Fig. 6, Supplementary Table S6 for all modelling results).

For the two first flood events, the <2 µm fraction of the carbonate source soil end-member had the highest contributions, estimated between 73% to the GB station and 100% to the BR station, to the suspended sediment collected in the carbonate area located in the southern part of the catchment. In the northern part of the catchment, the silicate soil contributions remained in the same order of magnitude during the two first flood events with respective mean silicate contributions of 59% and 52%. During the third flood event, the <2 mm silicate soil end-member contributed the most to suspended sediment with contributions ranging between 55% and 86%, with a mean contribution of 72%.

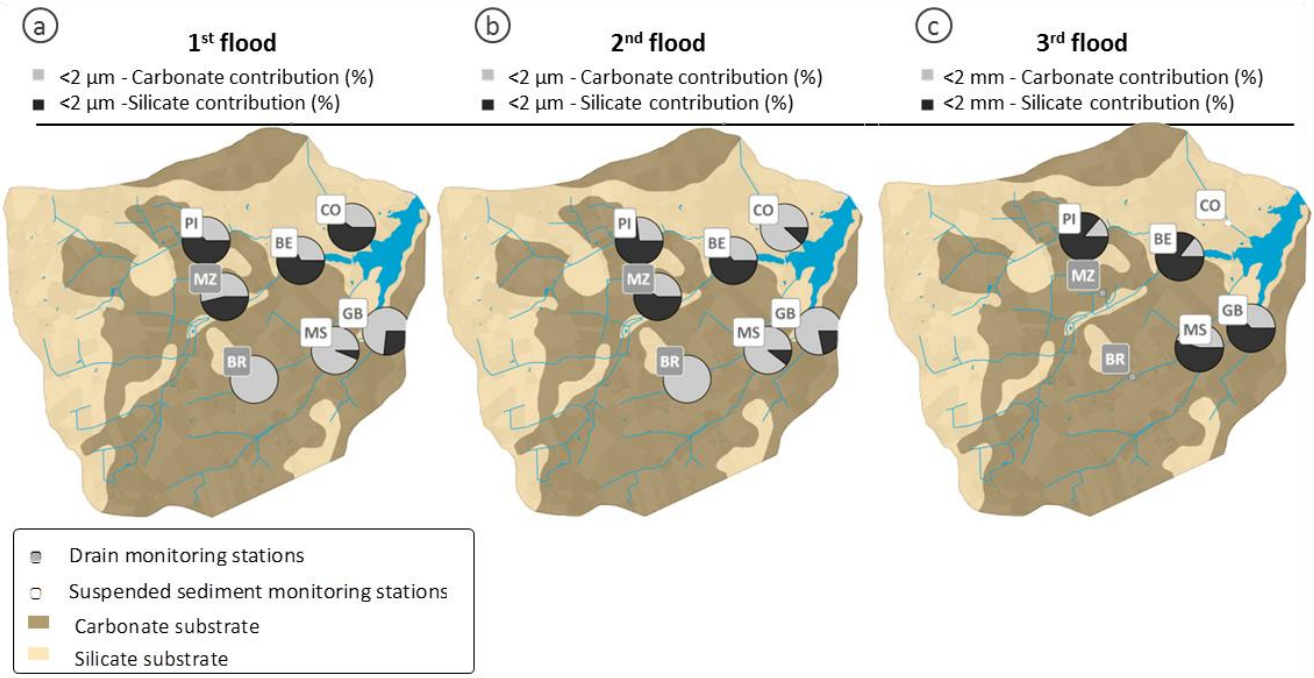

Figure 6. Carbonate and silicate soil contributions (%) to suspended sediment using $^{87}Sr/^{86}Sr$ ratios measured in the <2 µm fraction for the two first flood events (a and b) and in the <2 mm fraction for the third flood event (c).

4 Discussion

4.1 Temporal variability of suspended sediment characteristics and source effect

4.1.1 Impact of flood events on suspended sediment transport

In the Louroux catchment, suspended sediment concentrations and water discharge exhibited clockwise hysteresis loops during the three flood events. Hysteresis patterns characterize suspended sediment stock and exhaustion and are commonly used to investigate their sources during floods (Williams, 1989; Sherriff et al., 2016). Clockwise hysteresis loops suggest that suspended sediment originates from a close source and reflects the progressive decline in suspended sediment availability. They are commonly attributed to a depletion of available sediment before the maximum discharge is reached (Walling, 1977; Horowitz, 2008). Accordingly, suspended sediment transported in the Louroux catchment during the three flood events may correspond to material previously accumulated in the river bed and easily remobilized during the rising limb of the flood and/or to sediment that originated from eroded sources located relatively close to the monitoring stations.

Suspended sediment exported from local sources depends on the quantity of sediment previously stored in the river channels. In agricultural lowland catchments, higher suspended sediment concentrations may be observed in winter due to the higher sensitivity of soils to erosion during this season (Delmas et al., 2011). A previous study demonstrated that in the Louroux catchment, suspended sediment transported during floods almost exclusively originate from surface sources (Foucher et al., 2015), suggesting that the clockwise hysteresis loops observed may be attributed to the erosion of local surface sources, transiting the highly connected drainage network, rather than to the resuspension of channel bed sediment as observed in lowland catchments in the UK (Evans et al., 2003; Collins and Walling, 2006).

4.1.2 Source discrimination with $^{87}Sr/^{86}Sr$ ratios

$^{87}Sr/^{86}Sr$ ratios have been commonly used in sediment provenance studies in large river basins. However, less attention has been focused on local, small-scale catchments. Indeed, using $^{87}Sr/^{86}Sr$ ratios may be challenging at smaller scales because of potential local heterogeneities, which may be homogenized in larger scale research. In the Louroux catchment, $^{87}Sr/^{86}Sr$ ratios measured in soil and suspended sediment samples presented significant variations and highlighted the utility of using this tracer for tracing sediment source dynamics at smaller spatial scales.

In this study, $^{87}Sr/^{86}Sr$ ratios measured in soil and suspended sediment samples varied according to the particle size and to the hydrological conditions. As $^{87}Sr/^{86}Sr$ ratios measured in the suspended sediment did not plot along a mixing line between the carbonate and silicate <2 mm soil samples, Sr isotopic signatures were investigated in the <63 and <2 µm fractions of soil samples. When investigating $^{87}Sr/^{86}Sr$ ratios versus elemental ratios (K/Sr, Ca/Sr, 1/Sr, Rb/Sr), the <2 µm fraction of soil samples was shown to provide a more appropriate source for suspended sediment transported in the river network. Na/Sr ratios did not discriminate between the different soil fractions and suspended sediment samples. Indeed, the <2 µm fraction of soil samples was enriched in Na compared to suspended sediment samples (Supplementary Tables S3 and S5). These high concentrations may be explained by a supply in Na originating from the deionized water used to isolate the <2 µm particles. This contamination may have induced the crystallization of minerals containing Na on fine particles, such as clays, when the solutions with <2 µm particles were dried. Overall, the use of $^{87}Sr/^{86}Sr$ and Rb/Sr ratios provided the best discrimination between suspended sediment samples and between the different soil fractions. A clear discrimination between suspended sediment samples from the two first flood events with signatures similar to that of the <2 µm fraction of soil samples and suspended sediment from the third flood event with signatures similar to that of the <2 mm fraction of soil samples was observed (Fig. 7).

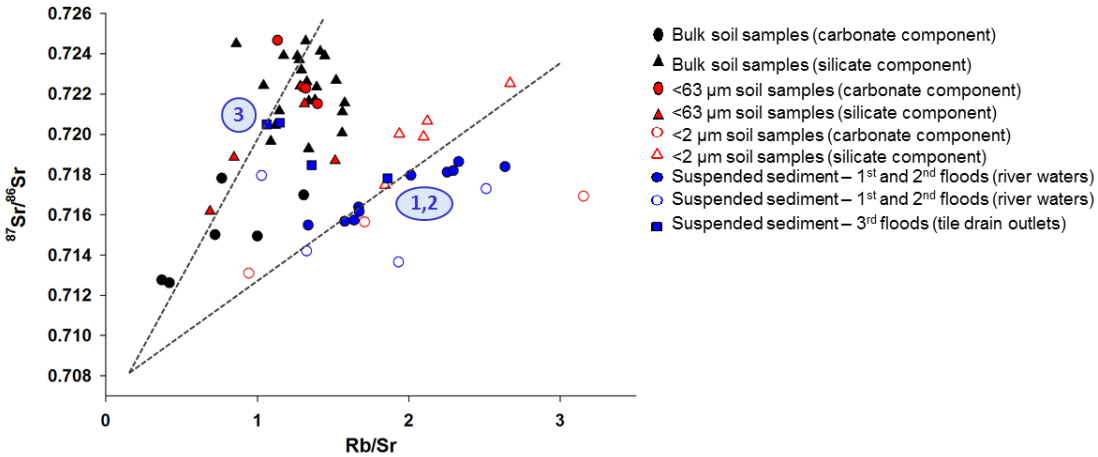

Figure 7. $^{87}Sr/^{86}Sr$ vs Rb/Sr in suspended sediment, carbonate and silicate soil samples (<2 mm, <63 µm and <2 µm fractions). 1,2,3: suspended sediment sampling campaign number.

These results indicate that in the Louroux catchment, suspended sediment collected during the two first floods, which plotted with the <2 µm fraction of soil samples, corresponded to fine particles whereas suspended sediment from the third flood, that plotted with <2 mm soil samples, corresponded to a coarser fraction. The particle size composition of fine sediment exerts a significant control on its mineralogy and geochemistry. According to Walling et al. (2000), material sieved to <2 µm will be mainly composed of primary or secondary silicate minerals, whereas larger particle size fractions will be dominated by quartz.

Results of the current research indicate that the <2 µm fraction of soil samples is characterized by a significant increase of the Rb/Sr ratios and a decrease or a stagnation of $^{87}Sr/^{86}Sr$ ratios compared to those measured in larger particle size fractions. These variations illustrate differences in the mineralogy of the analyzed particle size fractions. The increase of Rb/Sr ratios in the <2 µm fraction likely reflects an enrichment in secondary minerals, such as clays. However, to strengthen the Sr isotopic discrimination between the different particle size fractions of soils and the suspended sediment samples according to flood events, additional mineralogical analyses should be performed on the <2 µm, <63 µm and <2 mm fractions of soil samples, suspended sediment and separate minerals. The particle size distribution in soil samples should also be investigated to evaluate the proportion of the <2 µm fraction compared to the coarser fractions. Mineralogical and particle size measurements related to $^{87}Sr/^{86}Sr$ values could provide additional information, demonstrating that very fine particles were transported through this river network.

4.2 Variations in source contributions to suspended sediment and modelling implications

To estimate the relative contribution of the <2 µm and <2 mm fractions of carbonate and silicate soils to suspended sediment depending on the flood event, a mixing equation incorporating $^{87}Sr/^{86}Sr$ ratios and Sr concentrations was used. This approach illustrated the interest of conducting $^{87}Sr/^{86}Sr$ ratio measurements in different particle size fractions and under varying hydrological conditions. Although several studies have used geochemical properties (mostly major and trace element concentrations) in mixing models to estimate the contribution of different lithological sources (Olley and Caitcheon, 2000; Douglas et al., 2003; Evrard et al., 2011; Navratil et al., 2012b) or investigated the relation between the chemical and isotopic composition of the sediment transported under varying hydrological conditions and their particle size distribution (Bouchez et al., 2011a; Bouchez et al., 2011b; Lupker et al., 2011), fewer studies estimated sediment sources contributions after conducting geochemical measurements on different particle size fractions of source material (Navratil et al., 2012; Haddadchi et al., 2015).

The preliminary results obtained in the Louroux catchment showed the importance of modelling and estimating source contributions to the suspended sediment with different particle size fractions depending on the flood intensities. These results highlighted that sediment fingerprinting approaches conducted in this catchment and in other similar environments should target multiple particle size fractions: the <2 µm fraction in lower intensity events, and during more intense floods when a coarser fraction of sediment is transported, the <2 mm fraction of soil samples should be used to characterize the potential sources of sediment. Ultimately, the variations of Sr isotopic signatures observed in the different particle size fractions also indicated that $^{87}Sr/^{86}Sr$ ratios are not a straightforward tracer of sediment sources in this catchment. Indeed, the $^{87}Sr/^{86}Sr$ ratio must be traced across multiple particle size fractions in order to provide sediment source material. It is likely that there are other sediment fingerprint parameters that require a particle size fraction specific approach to accurately quantify sediment source dynamics.

4.3 Sediment transfer through the drainage network

The $^{87}Sr/^{86}Sr$ ratios were an effective tracer of suspended sediment sources when incorporating particle size. However, the specific role of the drainage network in the transport and the supply of sediment from tile drains to the river remains difficult to quantify. Sr isotopic measurements revealed that strong variations in signatures were observed in the different fractions of soils and in suspended sediment over the three flood events in the Louroux catchment. Hillslopes and drains mainly supplied very fine (clay-sized) particles to the rivers. Accordingly, the Sr isotopic signatures of suspended sediment coincided with the signatures of the <2

µm fraction of soil samples during the two first floods. The dense drainage system, with more than 220 tile drain outlets found across the catchment, could provide the main pathway for sediment delivery to the rivers during these events. These findings are consistent with the results obtained by Foucher et al. (2015), who found that sediment exported from the drains was modelled to originate almost exclusively from surface sources (99 ± 2.5%), suggesting that the drainage system facilitates the transfer of particles from the soil surface to the rivers in this cultivated catchment. The elevated contribution of the drainage system in the delivery of sediment to the rivers was also highlighted by other studies conducted in France and in the UK (Sogon et al., 1999; Russell et al., 2001; Walling et al., 2002). However, the migration of particles through the soil profile still remains poorly documented although the presence of macropores was suggested to provide a preferential pathway for particle transport in these drained environments (Walling et al., 2002; Jagercikova et al., 2014).

Sr isotopes were used to provide additional information on the sources of material transiting the drains. Lower $^{87}Sr/^{86}Sr$ ratios were observed between the <2 mm and <2 µm fractions of soil samples. $^{87}Sr/^{86}Sr$ ratios measured in suspended sediment collected at tile drain outlets were lower than the ratios measured in suspended sediment directly collected in the river and even lower for the BR station than most of the signatures measured in the <2 µm fraction of soil samples, suggesting that the material transiting the drain may be finer than 2 µm. These downward trends observed in $^{87}Sr/^{86}Sr$ ratios may indicate that particles transiting the drains are finer than most particles transported in the river. This is consistent with a previous study demonstrating that sediment exported by the drainage system was enriched in ^{137}Cs compared to soil samples. A significant particle size selection process likely occurs in the soil profile, with the migration of the finest particles through the drainage system (Foucher et al., 2014). Particle size measurements also showed that suspended sediment collected at tile drain outlets were very fine, with 50% of the particles having a diameter lower than 1 µm (S. Salvador-Blanes, unpublished results), which is consistent with our observations.

These results highlighted the importance of considering tile drains as a preferential source of sediment. The material transiting the drainage system and contributing to the supply of sediment to the rivers consists of very fine material (<2 µm) originating from surface soils. Accordingly, it is crucial to improve the management of the drain system in order to reduce the amount of sediment that they supply to the rivers. This is particularly true in winter, when flow from the drains is high and contributes significantly to sediment export.

5 Conclusions

This study highlighted the potential of Sr isotope measurements to identify suspended sediment sources and quantify their dynamics. $^{87}Sr/^{86}Sr$ ratios were used to discriminate between the potential sources of suspended sediment and to identify differences in their characteristics depending on flood intensity. $^{87}Sr/^{86}Sr$ ratios measured in suspended sediment varied in space and time reflecting changes in sources. The Sr isotopic signatures significantly varied in the different fractions of soil samples (i.e <2 mm, <63 µm, and <2 µm) and in suspended sediment, reflecting the preferential transfer of fine particles during sediment transport in the Louroux catchment. The particle size of sediment transiting the river network changes with hydrological conditions and our results suggest it may be important to fractionate source material to different particle sizes depending on flood intensity.

A preliminary modeling approach used $^{87}Sr/^{86}Sr$ ratios and Sr concentrations to estimate the relative contribution of sources to the suspended sediment. Results demonstrated that different particle size

fractions of sources can be used to estimate their respective contributions to the suspended sediment depending on hydrological conditions. Very fine sediment was shown to be exported from the tile drains, which demonstrates the need to better manage material supplied by tile drains to the river network. The creation of retention ponds could for instance trap this fine material and prevent it from reaching the river system.

These results highlighted the need to focus on the geochemical composition of soils instead of bedrock lithology to potentially better constrain sediment sources and pathways at the catchment scale in intensively cultivated environments. These investigations will improve our understanding of soil erosion processes and sediment supply in similar catchments. In the future, material separated to different particle size fractions could be used to identify the sources supplying sediment during floods of varying magnitude. For a better representativeness, suspended sediment should be monitored with high resolution sampling to characterize geochemical ($^{87}Sr/^{86}Sr$, elemental concentrations) and potential source variations over one single flood event. Additional radionuclide measurements (^{137}Cs, $^{210}Pb_{xs}$, ^{7}Be) should also be conducted in order to identify parameters that may help better discriminate the contribution of tile drain material to rivers.

Acknowledgements

This work received financial support from the Loire-Brittany Water Agency (TrackSed and Drastic projects). Marion Le Gall received a PhD fellowship from CEA (Commissariat à l'Energie Atomique et aux Energies Alternatives, France) and the DGA (Direction Générale de l'Armement, France), French MoD.

References

Albarède, F., 1995. Introduction to Geochemical Modeling. Cambridge University Press.

Allègre, C.J., Dupr, B., Philippe, N., Gaillardet, J., 1996. Sr-Nd-Pb isotope systematics in Amazon and Congo River systems : Constraints about erosion processes. Chemical Geology, 131: 93-112.

Asahara, Y., Tanaka, T., Kamioka, H., Nishimura, A., Yamazaki, T., 1999. Provenance of the north Pacific sediments and process of source material transport as derived from Rb–Sr isotopic systematics. Chemical Geology, 158: 271-291.

Audry, S., Schafer, J., Blanc, G., Jouanneau, J.M., 2004. Fifty-year sedimentary record of heavy metal pollution (Cd, Zn, Cu, Pb) in the Lot River reservoirs (France). Environmental Pollution, 132(3): 413-26.

Beusen, A.H.W., Dekkers, A.L.M., Bouwman, A.F., Ludwig, W., Harrison, J., 2005. Estimation of global river transport of sediments and associated particulate C, N, and P. Global Biogeochemical Cycles, 19(4).

Bouchez, J., Gaillardet, J., France-Lanord, C., Maurice, L., Dutra-Maia, P., 2011a. Grain size control of river suspended sediment geochemistry: Clues from Amazon River depth profiles. Geochemistry, Geophysics, Geosystems, 12(3).

Bouchez, J., Métivier, F., Lupker, M., Maurice, L., Perez, M., Gaillardet, J., France-Lanord, C., 2011b. Prediction of depth-integrated fluxes of suspended sediment in the Amazon River: particle aggregation as a complicating factor. Hydrological Processes, 25(5): 778-794.

Brennan, S.R., Fernandez, D.P., Mackey, G., Cerling, T.E., Bataille, C.P., Bowen, G.J., Wooller, M.J., 2014. Strontium isotope variation and carbonate versus silicate weathering in rivers from across Alaska: Implications for provenance studies. Chemical Geology, 389: 167-181.

Brenot, A., Baran, N., Petelet-Giraud, E., Négrel, P., 2008. Interaction between different water bodies in a small catchment in the Paris basin (Brévilles, France): Tracing of multiple Sr sources through Sr isotopes coupled with Mg/Sr and Ca/Sr ratios. Applied Geochemistry, 23(1): 58-75.

584 Chartin, C., Evrard, O., Onda, Y., Patin, J., Lefèvre, I., Ottlé, C., Ayrault, S., Lepage, H., Bonté, P., 2013. Tracking
585 the early dispersion of contaminated sediment along rivers draining the Fukushima radioactive
586 pollution plume. Anthropocene, 1: 23-34.
587 Collins, A.J., Walling, D.E., 2006. Investigating the remobilization of fine sediment stored on the channel bed
588 of lowland permeable catchments in the UK. Sediment Dynamics and the Hydromorphology of Fluvial
589 Systems (Proceedings of a symposium, IAHS): 471-479.
590 Collins, A.J., Walling, D.E., Leeks, G.J.L., 1997. Source type ascription for fluvial suspended sediment based on
591 a quantitative composite fingerprinting technique. Catena, 29: 1-27.
592 Collins, A.L., Zhang, Y., Walling, D.E., Grenfell, S.E., Smith, P., 2010. Tracing sediment loss from eroding farm
593 tracks using a geochemical fingerprinting procedure combining local and genetic algorithm
594 optimisation. Science of the Total Environment, 408(22): 5461-71.
595 Coynel, A., Schäfer, J., Blanc, G., Bossy, C., 2007. Scenario of particulate trace metal and metalloid transport
596 during a major flood event inferred from transient geochemical signals. Applied Geochemistry, 22(4):
597 821-836.
598 Delmas, M., Cerdan, O., Cheviron, B., Mouchel, J.M., 2011. River basin sediment flux assessments.
599 Hydrological Processes, 25(10): 1587-1596.
600 Douglas, G., Gray, C.M., Hart, B., Beckett, R., 1995. A strontium isotopic investigation of the origin of
601 suspended particulate matter (SPM) in the Murray-Darling River system, Australia. Geochimica et
602 Cosmochimica Acta, 59(18): 3799-3815.
603 Eikenberg, J., Tricca, A., Vezzu, G., Stille, P., Bajo, S., Ruethi, M., 2001. $^{228}Ra/^{226}Ra/^{224}Ra$ and $^{87}Sr/^{86}Sr$ isotope
604 relationship for determining intercations between ground and river water in the upper Rhine valley.
605 Journal of Environmental Radioactivity, 54: 133-162.
606 European Environment Agency, 2002. EEA-ETC/TE 2002. CORINE land cover update. I&CLC2000 project.
607 Technical Guidelines (http://terrestrial.eionet.eu.int).
608 Evans, D.J., Johnes, P., Lawrence, D.S., 2003. Suspended and bed load sediment transport dynamics in two
609 lowland UK streams—storm integrated monitoring. Erosion and sediment transport measurment in
610 rivers: technological and methodological advances. International Association of Hydrological Sciences:
611 103-110.
612 Evrard, O., Navratil, O., Ayrault, S., Ahmadi, M., Némery, J., Legout, C., Lefèvre, I., Poirel, A., Bonté, P.,
613 Esteves, M., 2011. Combining suspended sediment monitoring and fingerprinting to determine the
614 spatial origin of fine sediment in a mountainous river catchment. Earth Surface Processes and
615 Landforms, 36(8): 1072-1089.
616 Faure, G., 1986. Principles of Isotopic Geology. Wiley, New York.
617 Foucher, A., Laceby, J.P., Salvador-Blanes, S., Evrard, O., Le Gall, M., Lefevre, I., Cerdan, O., Rajkumar, V.,
618 Desmet, M., 2015. Quantifying the dominant sources of sediment in a drained lowland agricultural
619 catchment: the application of a thorium-based particle size correction in sediment fingerprinting.
620 Geomorphology.
621 Foucher, A., Salvador-Blanes, S., Evrard, O., Simonneau, A., Chapron, E., Courp, T., Cerdan, O., Lefèvre, I.,
622 Adriaensen, H., Lecompte, F., Desmet, M., 2014. Increase in soil erosion after agricultural
623 intensification: Evidence from a lowland basin in France. Anthropocene, 7: 30-41.
624 Gaillardet, J., Dupré, B., Allègre, C.J., Negrel, P., 1997. Chemical and physical denudation in the Amazon River
625 Basin. Chemical Geology, 142: 141-173.
626 Gateuille, D., Evrard, O., Lefevre, I., Moreau-Guigon, E., Alliot, F., Chevreuil, M., Mouchel, J.M., 2014. Mass
627 balance and decontamination times of Polycyclic Aromatic Hydrocarbons in rural nested catchments
628 of an early industrialized region (Seine River basin, France). Science of the Total Environment, 470-
629 471: 608-17.
630 Gay, A., Cerdan, O., Delmas, M., Desmet, M., 2014. Variability of suspended sediment yields within the Loire
631 river basin (France). Journal of Hydrology, 519: 1225–1237.
632 Gourdin, E., Evrard, O., Huon, S., Lefèvre, I., Ribolzi, O., Reyss, J.-L., Sengtaheuanghoung, O., Ayrault, S., 2014.
633 Suspended sediment dynamics in a Southeast Asian mountainous catchment: Combining river
634 monitoring and fallout radionuclide tracers. Journal of Hydrology, 519: 1811-1823.

635 Graustein, W.C., 1989. $^{87}Sr/^{86}Sr$ ratios measure the sources and flow of strontium in terrestrial environment.
636 In: Springer, N.-Y. (Ed.), Stable Isotopes in Ecological Research, pp. 491-512.
637 Grosbois, C., Negrel, P., Fouillac, C., Grimaud, D., 1999. Dissolved load of the Loire River: chemical and
638 isotopic characterization. Chemical Geology, 170(1-4): 179-201.
639 Haddadchi, A., Olley, J., Pietsch, T., 2015. Variable source contributions to river bed sediments across three
640 size fractions. Hydrological Processes.
641 Horowitz, A.J., 2008. Determining annual suspended sediment and sediment-associated trace element and
642 nutrient fluxes. Science of the Total Environment, 400(1-3): 315-43.
643 Jagercikova, M., Cornu, S., Le Bas, C., Evrard, O., 2014. Vertical distributions of ^{137}Cs in soils: a meta-analysis.
644 Journal of Soils and Sediments, 15(1): 81-95.
645 King, K.W., Fausey, N.R., Williams, M.R., 2014. Effect of subsurface drainage on streamflow in an agricultural
646 headwater watershed. Journal of Hydrology, 519: 438-445.
647 Koiter, A.J., Owens, P.N., Petticrew, E.L., Lobb, D.A., 2013. The behavioural characteristics of sediment
648 properties and their implications for sediment fingerprinting as an approach for identifying sediment
649 sources in river basins. Earth-Science Reviews, 125: 24-42.
650 Laceby, J.P., Olley, J., Pietsch, T.J., Sheldon, F., Bunn, S.E., 2015. Identifying subsoil sediment sources with
651 carbon and nitrogen stable isotope ratios. Hydrological Processes, 29(8): 1956-1971.
652 Liu, Y., Métivier, F., Gaillardet, J., Ye, B., Meunier, P., Narteau, C., Lajeunesse, E., Han, T., Malverti, L., 2011.
653 Erosion rates deduced from seasonal mass balance along the upper Urumqi River in Tianshan. Solid
654 Earth, 2(2): 283-301.
655 Lupker, M., France-Lanord, C., Lavé, J., Bouchez, J., Galy, V., Métivier, F., Gaillardet, J., Lartiges, B., Mugnier, J.-
656 L., 2011. A Rouse-based method to integrate the chemical composition of river sediments:
657 Application to the Ganga basin. Journal of Geophysical Research, 116(F4).
658 Navratil, O., Evrard, O., Esteves, M., Ayrault, S., Lefèvre, I., Legout, C., Reyss, J.-L., Gratiot, N., Némery, J.,
659 Mathys, N., Poirel, A., Bonté, P., 2012. Core-derived historical records of suspended sediment origin
660 in a mesoscale mountainous catchment: the River Bléone, French Alps. Journal of Soils and
661 Sediments, 9(1-16).
662 Négrel, P., Allègre, C.J., Dupré, B., Lewin, E., 1993. Erosion sources determined by inversion of major and trace
663 elment ratios and strontium isotopic ratios in river water: The Congo Basin case. Earth and Planetary
664 Science Letters, 120: 59-76.
665 Négrel, P., Petelet-Giraud, E., 2004. Strontium isotopes as tracers of groundwater-induced floods: the Somme
666 case study (France). Journal of Hydrology, 305(1-4): 99-119.
667 Ollivier, P., Radakovitch, O., Hamelin, B., 2011. Major and trace element partition and fluxes in the Rhône
668 River. Chemical Geology, 285(1-4): 15-31.
669 Owens, P.N., Batalla, R.J., Collins, A.J., Gomez, B., Hicks, D.M., Horowitz, A.J., Kondolf, G.M., Marden, M.,
670 Page, M.J., Peacock, D.H., Petticrew, E.L., Salomons, W., Trustrum, N.A., 2005. Fine-grained sediment
671 in river systems: environmental significance and management issues. River Research and
672 Applications, 21(7): 693-717.
673 Petelet-Giraud, E., Négrel, P., 2007. Geochemical flood deconvolution in a Mediterranean catchment (Hérault,
674 France) by Sr isotopes, major and trace elements. Journal of Hydrology, 337(1-2): 224-241.
675 Pierson-Wickmann, A.-C., Aquilina, L., Weyer, C., Molénat, J., Lischeid, G., 2009. Acidification processes and
676 soil leaching influenced by agricultural practices revealed by strontium isotopic ratios. Geochimica et
677 Cosmochimica Acta, 73(16): 4688-4704.
678 Priadi, C., Bourgeault, A., Ayrault, S., Gourlay-France, C., Tusseau-Vuillemin, M.H., Bonte, P., Mouchel, J.M.,
679 2011. Spatio-temporal variability of solid, total dissolved and labile metal: passive vs. discrete
680 sampling evaluation in river metal monitoring. Journal of Environmental Monitoring, 13(5): 1470-9.
681 Probst, A., El Gh'mari, D., Aubert, D., Fritz, B., McNutt, R., 2000. Strontium as a tracer of weathering processes
682 in a silicate catchment polluted by acid atmospheric inputs, Strengbach, France. Chemical Geology,
683 170: 203-219.
684 Rasplus, L., Macaire, J.J., Alcaydé, G., 1982. Carte géologique de Bléré au 1:5000, Editions BRGM.

685 Roy, S., Gaillardet, J., Allègre, C.J., 1999. Geochemistry of dissolved and suspended loads of the Seine river,
686 France: Anthropogenic impact, carbonate and silicate weathering. Geochimica et Cosmochimica Acta,
687 63(9): 1277-1292.
688 Russell, R., Walling, D.E., Hodgkinson, R.A., 2001. Suspended sediment sources in two small lowland
689 agricultural catchments in the UK. Journal of Hydrology, 252(1-4): 1-24.
690 Semhi, K., Clauer, N., Probst, J.L., 2000. Strontium isotope compositions of river waters as records of
691 lithology-dependet mass transfers: the Garonne river and its tributaries (SW France). Chemical
692 Geology, 168: 173-193.
693 Sherriff, S.C., Rowan, J.S., Fenton, O., Jordan, P., Melland, A.R., Mellander, P.-E., hHallacháin, Ó., 2016. Storm
694 Event Suspended Sediment-Discharge Hysteresis and Controls in Agricultural Watersheds:
695 Implications for Watershed Scale Sediment Management. Environmental Science & Technology,
696 50(4): 1769-1778.
697 Smith, H.G., Blake, W.H., 2014. Sediment fingerprinting in agricultural catchments: A critical re-examination of
698 source discrimination and data corrections. Geomorphology, 204: 177-191.
699 Smith, H.G., Dragovich, D., 2009. Interpreting sediment delivery processes using suspended sediment-
700 discharge hysteresis patterns from nested upland catchments, south-eastern Australia. Hydrological
701 Processes, 23(17): 2415-2426.
702 Sogon, S., Penven, M.-J., Bonte, P., Muxart, T., 1999. Estimation of sediment yield and soil loss using
703 suspended sediment load and ^{137}Cs measurements on agricultural land, Brie Plateau, France.
704 Hydrobiologia, 410(251-261).
705 Vanmaercke, M., Poesen, J., Govers, G., Verstraeten, G., 2015. Quantifying human impacts on catchment
706 sediment yield: A continental approach. Global and Planetary Change, 130: 22-36.
707 Verstraeten, G., Poesen, J., 1999. The nature of small-scale flooding, muddy floods and retention pond
708 sedimentation in central Belgium. Geomorphology, 29: 275–292.
709 Viers, J., Dupre, B., Gaillardet, J., 2009. Chemical composition of suspended sediments in World Rivers: New
710 insights from a new database. Science of the Total Environment, 407(2): 853-68.
711 Walling, D.E., 1977. Assessing the accuracy of suspended sediment rating curves for a small bassin. Water
712 Resource Research, 13: 531-538.
713 Walling, D.E., Collins, A.L., 2008. The catchment sediment budget as a management tool. Environmental
714 Science & Policy, 11(2): 136-143.
715 Walling, D.E., Fang, D., 2003. Recent trends in the suspended sediment loads of the world's rivers. Global and
716 Planetary Change, 39(1-2): 111-126.
717 Walling, D.E., Owens, P.N., Waterfall, B.D., Graham, J.L., Wass, P.D., 2000. The particle size characteristics of
718 fluvial suspended sediment in the Humber and Tweed catchments, UK. Science of the Total
719 Environment, 251/252: 205-222.
720 Walling, D.E., Russell, R., Hodgkinson, R.A., Zang, Y., 2002. Establishing sediment budgets for two small
721 lowland agricultural catchments in the UK. Catena, 47: 323-353.
722 Williams, G.P., 1989. Sediment concentration versus water discharge during single hydrologic events in rivers.
723 Journal of Hydrology, 111(1-4): 89-106.
724 World Reference Base for Soil Resources, 2006. A framework for international classification, correlation and
725 communication. Food and Agriculture Organization of the United Nations - FAO. IUSS Working Group
726 WRB. World Soil Resources Reports No. 103, Rome, Italy.
727
728
729
730
731
732

Supplementary material

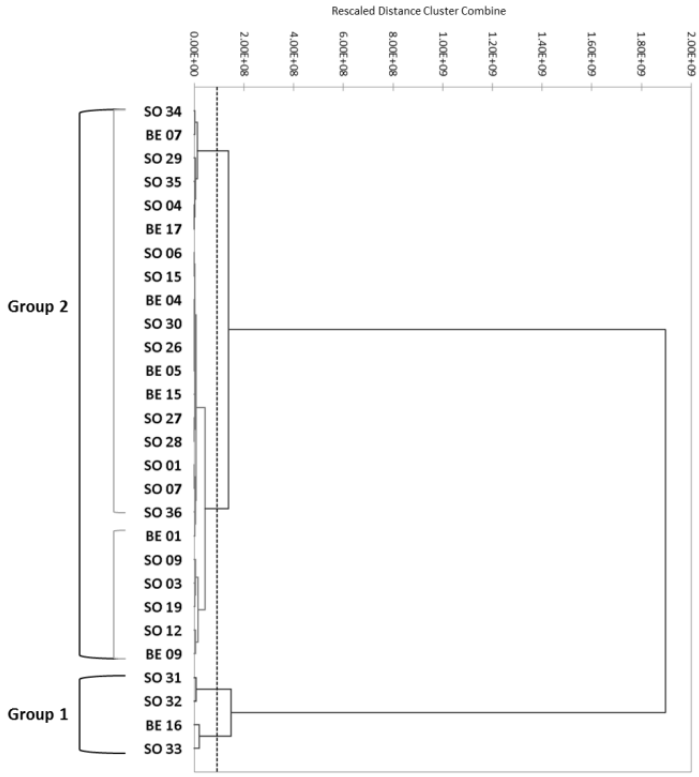

Figure S1. Dendogram of the hierarchical cluster analysis based on $^{87}Sr/^{86}Sr$ ratios, Na, Mg, K, Ca, Rb and Sr concentration measured in source samples.

Table S1. Summary of $^{87}Sr/^{86}Sr$ ratios, element concentrations (mg kg^{-1}) and 1/Sr and Rb/Sr ratios in soil samples.

Sample ID	Latitude (°N)	Longitude (°E)	$^{87}Sr/^{86}Sr$	± 2σ	Na (mg kg^{-1})	Mg (mg kg^{-1})	K (mg kg^{-1})	Ca (mg kg^{-1})	Rb (mg kg^{-1})	Sr (mg kg^{-1})	1/Sr	Rb/Sr
SO 01	47.151	0.76	0.722426	0.000013	3883	1184	9845	2289	52	50	0.020	1.04
SO 03	47.145	0.747	0.721704	0.000012	3259	3041	12879	5577	98	71	0.014	1.38
SO 04	47.144	0.743	0.723706	0.000005	1772	795	6047	1782	37	29	0.034	1.26
SO 06	47.138	0.729	0.723199	0.000012	4226	1839	12473	2725	80	62	0.016	1.29
SO 07	47.122	0.738	0.724631	0.000008	4419	1155	10681	2108	62	47	0.021	1.32
SO 09	47.13	0.757	0.719287	0.000048	2703	4004	13028	7021	99	74	0.013	1.33
SO 12	47.141	0.771	0.714943	0.000006	3403	4631	9972	4002	98	98	0.010	1.00
SO 15	47.149	0.723	0.724506	0.000006	4289	1442	12125	3363	43	50	0.020	0.85
SO 19	47.158	0.739	0.721115	0.000006	2952	3059	13910	4110	114	73	0.014	1.56
SO 26	47.127	0.771	0.723899	0.000006	3075	1889	11595	2012	78	54	0.019	1.44
SO 27	47.156	0.770	0.723910	0.000006	3064	1883	11555	2885	68	58	0.017	1.17
SO 28	47.138	0.723	0.721561	0.000007	3002	1845	11321	3413	104	66	0.015	1.58
SO 29	47.129	0.723	0.72388	0.000019	1352	538	4103	642	24	19	0.054	1.28
SO 30	47.119	0.731	0.724116	0.000008	3360	1381	11093	2267	75	53	0.019	1.42
SO 31	47.139	0.772	0.716986	0.000006	4537	4594	10253	20192	94	72	0.014	1.30
SO 32	47.138	0.758	0.712763	0.000008	1965	1997	8929	20897	56	152	0.007	0.37
SO 33	47.14	0.764	0.715012	0.000008	3056	3103	8701	35698	67	93	0.011	0.72
SO 34	47.137	0.757	0.722388	0.000008	1083	1086	8092	2469	50	39	0.026	1.27
SO 35	47.135	0.753	0.717815	0.000008	1230	1242	6701	2754	39	51	0.020	0.76
SO 36	47.136	0.754	0.721163	0.000008	1860	1885	10847	3404	71	62	0.016	1.15
BE 01	47.151	0.760	0.720446	0.000049	3245	2018	10077	3246	66	59	0.017	1.12
BE 04	47.138	0.729	0.722606	0.000049	3924	1935	12158	1934	84	63	0.016	1.33
BE 05	47.124	0.744	0.722340	0.000049	3393	1841	11834	2473	85	61	0.016	1.39
BE 07	47.131	0.759	0.719653	0.000008	2377	1516	8809	2873	58	54	0.019	1.09
BE 09	47.141	0.771	0.720070	0.000049	3090	3937	9672	6857	82	53	0.019	1.56
BE 15	47.130	0.733	0.722685	0.000005	2820	2856	12165	2692	93	61	0.016	1.52
BE 16	47.138	0.761	0.712625	0.000006	2867	2808	10527	29632	74	177	0.006	0.42
BE 17	47.154	0.740	0.721651	0.000005	1626	1352	5981	1956	65	48	0.021	1.34

Table S2. $^{7}Sr/^{86}Sr$ ratios, elemental concentrations (mg kg^{-1}), 1/Sr and Rb/Sr ratios in SPM collected in the rivers (Conteraye, Picarderie, Beaulieu, Masniers, Grand Bray) and at tile drain outlets (Mazère, Brépinnière) during three flood events.

Flood event Localisation	Suspended sediment concentration (mg/L)	$^{87}Sr/^{86}Sr$	± 2σ	Na (mg kg^{-1})	Mg (mg kg^{-1})	Al (mg kg^{-1})	K (mg kg^{-1})	Ca (mg kg^{-1})	Rb (mg kg^{-1})	Sr (mg kg^{-1})	1/Sr	Rb/Sr
Suspended sediment - 1st flood event (12/30/2013)												
Conteraye	270	0.717964	0.000012	2338	5378	90028	14480	6081	157	78	0.013	2.01
Picarderie	335	0.718114	0.000013	1040	6760	102146	14320	7055	173	77	0.013	2.25
Beaulieu	414	0.718384	0.000009	900	6894	102495	13085	7311	178	68	0.015	2.64
Masniers	337	0.715484	0.000014	1896	6379	86433	14957	22546	163	122	0.008	1.34
Grand Bray	386	0.716377	0.000013	1477	7293	108179	17009	14457	191	114	0.009	1.67
Mazère	324	0.717296	0.000014	972	7582	111628	15390	7445	196	78	0.013	2.51
Brépinière	300	0.714202	0.000013	1095	6860	101125	14511	8341	166	126	0.008	1.33
Suspended sediment - 2nd flood event (01/29/2014)												
Conteraye	40	0.715734	0.000014	257	5738	94320	12207	12353	159	97	0.010	1.64
Picarderie	167	0.718637	0.000014	624	7325	117421	15557	12190	193	83	0.012	2.33
Beaulieu	219	0.718188	0.000013	340	7441	113307	15890	11292	197	86	0.012	2.29
Masniers	107	0.715671	0.000016	780	6850	95783	14873	7629	177	113	0.009	1.56
Grand Bray	133	0.716165	0.000014	917	6723	98741	15345	11385	178	107	0.009	1.67
Mazère	68	0.717946	0.000013	n.d	5911	91574	11741	17278	69	68	0.015	1.03
Brépinière	124	0.713660	0.000012	496	6103	97440	13298	12232	233	121	0.008	1.93
Suspended sediment - 3rd flood event (02/13/2014)												
Picarderie	774	0.720571	0.000011	1636	3969	56006	14137	7095	71	62	0.016	1.15
Beaulieu	813	0.720495	0.000012	n.d	3529	54384	13871	5425	65	61	0.016	1.06
Masniers	470	0.717814	0.000012	2018	6291	88825	16062	11935	167	90	0.011	1.86
Grand Bray	541	0.718467	0.000012	1958	5852	77427	16726	9810	109	80.4	0.012	1.36

Table S3. $^{87}Sr/^{86}Sr$ ratios, Sr and Rb concentrations (mg kg^{-1}) in various particle size fractions of the soil samples.

Sample ID		$^{87}Sr/^{86}Sr$	Sr (mg kg^{-1})	Rb (mg kg^{-1})
SO 03		0.721704	71	98
SO 03 <63 µm	Silicate soils	0.722356	76	99
SO 03 <2 µm		0.719877	72	151
SO15		0.724506	50	43
SO15 <63 µm	Silicate soils	0.724667	65	73
SO15 <2 µm		0.722535	58	155
SO 19		0.721115	73	114
SO 19 <63 µm	Silicate soils	0.721521	77	106
SO 19 <2 µm		0.720018	77	149
SO 28		0.721561	60	104
SO 28 <63 µm	Silicate soils	0.722288	72	95
SO 28 <2 µm		0.720653	75	159
SO 31		0.716986	72	94
SO 31 <63 µm	Carbonate soils	0.718687	73	110
SO 31 <2 µm		0.716922	56	177
SO 33		0.715012	93	67
SO 33 <63 µm	Carbonate soils	0.716178	101	70
SO 33 <2 µm		0.715645	81	138
SO 35		0.717815	51	39
SO35 <63 µm	Carbonate soils	0.718855	82	69
SO35 <2 µm		0.713099	120	114
SO 36		0.721163	62	71
SO 36 <63 µm	Silicate soils	0.721510	72	94
SO 36 <2 µm		0.717482	84	155

Table S4. $^{87}Sr/^{86}Sr$ ratios, element concentrations (mg kg^{-1}), 1/Sr and Rb/Sr ratios in the fraction <63 µm of eight soil samples.

Sample ID	$^{87}Sr/^{86}Sr$	± 2σ	Na (mg kg^{-1})	Mg (mg kg^{-1})	K (mg kg^{-1})	Ca (mg kg^{-1})	Rb (mg kg^{-1})	Sr (mg kg^{-1})	1/Sr (mg kg^{-1})	Rb/Sr (mg kg^{-1})
SO 03 <63 µm	0.722356	0.00001	3966	2951	14850	5998	99	76	0.013	1.30
SO 15 <63 µm	0.724667	0.00001	5233	1395	14373	2791	73	65	0.016	1.13
SO 19 <63 µm	0.721521	0.00001	2300	2839	14741	4232	108	77	0.013	1.40
SO 28 <63 µm	0.722288	0.00001	3825	2403	14426	3776	95	72	0.014	1.32
SO 31 <63 µm	0.718687	0.00001	3804	4901	13282	25472	110	73	0.014	1.51
SO 33 <63 µm	0.716178	0.00000	4160	3892	12255	63573	70	101	0.010	0.69
SO 35 <63 µm	0.718855	0.00001	5096	1893	13136	4992	69	82	0.012	0.85
SO 36 <63 µm	0.721510	0.00001	5056	2141	14641	4266	94	72	0.014	1.31

Table S5. $^{87}Sr/^{86}Sr$ ratios, elemental concentrations (mg kg^{-1}), 1/Sr and Rb/Sr ratios in the clay fraction (<2 µm) of eight soil samples.

Sample ID	$^{87}Sr/^{86}Sr$	± 2σ	Na (mg kg^{-1})	Mg (mg kg^{-1})	K (mg kg^{-1})	Ca (mg kg^{-1})	Rb (mg kg^{-1})	Sr (mg kg^{-1})	1/Sr	Rb/Sr
SO 03<2 µm	0.719877	0.000043	49570	5460	14649	7945	151	72	0.014	2.10
SO 15<2 µm	0.722535	0.000043	67941	5099	14183	6859	155	58	0.017	2.67
SO 19<2 µm	0.720018	0.000043	45653	4577	15164	5570	148	77	0.013	1.94
SO 28<2 µm	0.720653	0.000039	39246	5044	15826	5502	159	75	0.013	2.12
SO 31<2 µm	0.716922	0.000039	46947	9679	13364	14842	177	56	0.018	3.15
SO 33<2 µm	0.715645	0.000039	64399	6156	14752	11969	138	81	0.012	1.71
SO 35<2 µm	0.713099	0.000039	56543	5423	12900	10569	114	120	0.008	0.94
SO 36<2 µm	0.717482	0.000039	55603	5550	14229	6487	155	84	0.012	1.84

794 **Table S6. Relative contributions of the silicate and carbonate end-members to the suspended sediment during three flood events.**

Samples	Carbonate contribution (%)	Silicate contribution (%)
1st flood event (<2 µm fraction)		
Grand Bray (GB1)	73	27
Masniers (MS1)	94	6
Brépinière (BR1)	100	0
Conteraye (CO1)	40	60
Beaulieu (BE1)	32	68
Picarderie (PI1)	37	63
Mazère (MZ1)	54	46
2nd flood event (<2 µm fraction)		
Grand Bray (GB2)	78	22
Masniers (MS2)	89	11
Brépinière (BR2)	100	0
Conteraye (CO2)	88	12
Beaulieu (BE2)	36	64
Picarderie (PI2)	27	73
Mazère (MZ2)	40	60
3rd flood event (<2 mm fraction)		
Grand Bray (GB3)	36	64
Masniers (MS3)	45	55
Beaulieu (BE3)	15	85
Picarderie (PI3)	14	86

795